
Article:
Dong, H. orcid.org/0000-0001-8025-4120, Tian, Z. orcid.org/0000-0001-7295-3327, Spencer, J.W. et al. (2 more authors) (2023) Coordinated Control Strategy of Railway Multisource Traction System With Energy Storage and Renewable Energy. IEEE Transactions on Intelligent Transportation Systems, 24 (12). pp. 15702-15713. ISSN 1524-9050

https://doi.org/10.1109/tits.2023.3271464

Coordinated Control Strategy of Railway Multi-Source Traction System with Energy Storage and Renewable Energy

Hongzhi Dong, *Student Member, IEEE*, Zhongbei Tian *Member, IEEE*, Joseph W. Spencer, David Fletcher, Siavash Hajiabady

***Abstract*— Influenced by the growing daily travel demand of citizens and extension of urban land, the construction of the urban railway transit (URT) system is gradually increasing nowadays. This situation implies more electricity consumption in URT and more challenges to URT operation stability. Therefore, based on the existing traction substation, this research proposes a configuration of multi-source traction system (MSTS) for URT with a coordinated control strategy according to power profile of the system. The proposed MSTS, including conventional traction system (CTS), renewable energy source (RES), and energy storage system (ESS), have been modelled first. After that, considering the system dynamic performance and ESS capacity, a coordinated control strategy is designed to manage the MSTS energy flow. The control strategy considers the substation voltage as control signal which is optimized by proposed performance index. The case study is conducted on a three-station railway route with two substations. The proposed MSTS with a coordinated control strategy is compared with normal CTS considering multi-train timetables with different departure intervals. The simulation result illustrates that the proposed MSTS can maintain the state of charge (SOC) of ESS and reduce the substation peak power and voltage fluctuation, which is verified both in short-term and long-term simulation. Meanwhile, it can improve the substation capacity by decreasing the energy consumption of CTS to deal with the increasing demand for URT. the case study denotes that the energy-saving rate can be up to 36.25%, and the peak power is reduced up to 46.32%.**

***Index Terms*—Urban railway transit, energy storage system, coordinated control strategy**

NOMENCLATURE

Variables

v	Train velocity
s	Train position
m_{eq}	Train equivalent mass
m_0	Empty train mass
m_l	Load mass
λ	Dimensionless rotating mass factor
F_{veh}	Train traction force
F_r	Train resistance force
k_0, k_1, k_2	Resistance coefficients
P_{me}	Train mechanical power
P_{el}	Train electrical power
U_l	Catenary voltage
η	Traction chain conversion efficiency
U_{sub}	Substation voltage
U_{OC}	Substation no-load voltage
I_{sub}	Substation current
R_{sub}	Substation resistance
U_C	Capacitor voltage
C_{SC}	Capacitance
I_{SC}	Capacitor current
U_{SC}	Supercapacitor voltage
R_C	Supercapacitor resistance
I_{SC}	Supercapacitor current
U_{ESS}	ESS voltage
I_{ESS}	ESS current
SOC	ESS state of charge
SOC_{max}	Maximum ESS state of charge
SOC_{min}	Minimum ESS state of charge
U_{cn}	Supercapacitor nominal voltage
P_{ESS_dismax}	ESS maximum discharge power
P_{ESS_chmax}	ESS maximum charge power
U_1-U_6	Voltage signal of ESS work state
P_{tb}	Reused RBE power
P_b	Total RBE power
P_{br}	RBE consumed in braking resistance
P_{sub}	Substation power
P_{RBE}	Rbe
J	System performance index
P_{sub_os}	Substation power overshoot

This research is supported by the EPSRC (grant reference EP/S032053/1) . The corresponding author is Zhongbei Tian.

Hongzhi Dong is with the Department of Electrical Engineering and Electronics, University of Liverpool, Liverpool, U.K. (e-mail: Hongzhi.dong@liverpool.ac.uk).

Zhongbei Tian is with the Department of Electrical Engineering and Electronics, University of Liverpool, Liverpool, U.K. (e-mail: Zhongbei.tian@liverpool.ac.uk).

Joseph W. Spencer is with the Department of Electrical Engineering and Electronics, University of Liverpool, Liverpool, U.K. (e-mail: Joe@liverpool.ac.uk).

David Fletcher is with the Department of Mechanical Engineering, University of Sheffield, Sheffield, U.K. (e-mail: D.I.Fletcher@Sheffield.ac.uk).

Siavash Hajiabady is currently a Distribution Engineer at the Network Rail, UK (e-mail: Siavash.Hajiabady@networkrail.co.uk)

P_{sub_up}	Substation power overshoot benchmark
U_{sub_os}	Substation voltage overshoot
U_{sub_us}	Substation voltage undershoot
U_{sub_up}	Substation voltage overshoot benchmark
U_{sub_down}	Substation voltage undershoot benchmark
i	Substation number
n	Total number of substations
t	System operation time t
T	Total system operation time
P_{peak}	Peak power of substation
U_{t_rate}	Train rated voltage
P_{au}	Auxiliary power

Abbreviation

URT	Urban railway system
MSTS	Multi-source traction system
RBE	Regenerative braking energy
ESS	Energy storage system
RES	Renewable energy source
CTS	Conventional traction system
SOC	State of charge
SC	Supercapacitor

I. Introduction

Urban railway transit (URT) is the most convenient and safe mode of transportation within cities. However, URT consumes a large quantity of electricity nowadays, as it has become an efficient method to reduce the carbon emission caused by fuel vehicles in most large-scale cities [1, 2]. At the end of 2019, 40 cities had been equipped with urban railway systems in China. The total length of the railway was up to 6,736.2 km, which consumed 152.6×10^9 kWh of electricity [3], and this trend of increase in energy consumption will rise continuously with the increasing demand for transportation and the expansion of modern cities [4]. Besides, the demand for higher speed and more carrying capacity in the railway system requires much more electricity. Thus, the study on the improvement of energy efficiency should be deeply investigated, especially via renewable energy sources (RES) and energy storage systems (ESS).

One of the technical routes to improving energy efficiency is optimizing the timetable and driving profile of the URT. Timetable optimization increases the overlapping time between accelerating train and braking train and then transfers the regenerative braking energy (RBE) to the traction trains [5]. In [6], researchers proposed a cooperative scheduling approach to optimize overlapping time, improving the utilization of RBE. Besides, other objectives are also taken into account with the timetable. In [7], both timetable and passenger waiting time were considered, while the operation cost and timetable were optimized together [8]. In terms of driving profile optimization, the main objective is to minimize mechanical energy consumption [9, 10]. Researchers optimized train speed profiles based on the maximum-minimum ant system algorithm, reducing the total traction energy in [11]. [12] analyzed different approaches such as genetic algorithm, ant colony optimization, and dynamic programming for the optimization of eco-driving method. Furtherly, [13] considers both timetable and speed profiles of train optimization to reduce energy consumption. A similar method can be seen in [14], authors proposed an eco-driving optimization for a single train and timetable optimization for the whole system. Besides, another eco-driving model which considers g the uncertainty of climatological conditions is established in [15], reducing 34.7% energy consumption. However, facing the increasing demand for transportation, this timetable and driving optimization method has a limited performance of energy consumption reduction and receptivity improvement of RBE.

ESS provides a potential approach to improve the utilization of RBE and the energy efficiency of URT, via storing and reusing the RBE, which is generally dissipated in brake resistance in URT. Meanwhile, ESS can also decrease the railway system's peak traction power demand. Researchers have proved the validity of RBE reutilization via ESS and its effect on reducing CO_2 emission [16]. The siting and sizing optimization of ESS is also a key problem in DC railway system [17]. The researchers proposed a cost model to optimize the ESS installation, obtaining a benefit of 188% the initial investment [18]. Together with timetable optimization, [19] utilized a nonlinear integer programming model to maximize the utilization of RBE. [4, 20] both investigated the URT with ESS and optimized the system configuration via genetic algorithms, which achieved a 15%-30% reduction in traction power consumption. Reference [21] proposed an energy transfer strategy and SOC tracking method, optimizing the discharging threshold of ESS and reducing the peak power of traction substation. [22] investigated the effect of ESS charging threshold on URT energy flow. [23] designed converter control strategy for ESS and optimized dynamic performance of the ESS. Furtherly, [24] proposed distributed cooperative control strategy for URT with ESS based on a value decomposition network, while [25] designed energy management for URT and optimized the charging threshold of ESS by deep reinforcement learning, improving the utilization of RBE. [26] designed a smart control strategy for ESS and RBE in URT system, reducing the energy consumption of substation. However, ESS can only improve the utilization rate of RBE but generate no additional energy to supply the traction substations.

RES like wind power (WP) and photovoltaic (PV) power, which can be installed in railway stations or on the rooftop of train vehicles, is capable of providing traction power or supporting auxiliary facilities [27]. Usually, the ESS also plays an indispensable role in URT with RES, eliminating the uncertainty of RES and charged by RES, which requires efficient control strategy and management. A basic structure of DC railway with ESS and RES is proposed in [28], which provides a foundation for further research. In the URT system equipped with ESS and RES, [29] and [30] proposed a day-ahead, minute-ahead, and real-time optimization for the system, which reduces the cost, energy consumption, and peak power of substations. In terms of control strategy, [31] proposed a self-adaptive control method for railway microgrid, including RES and ESS. The ESS will store extra energy from RES and transfer it to railway system when RES power is low. The RES uncertainty will affect the operation stability directly, and ESS charging and discharging actions needs to consider the RES uncertainty, ensuring that ESS has enough SOC to provide

traction power. The control strategy of URT system equipped with ESS and RES is still a challenge considering the uncertainty of RES and ESS limited capacity.

Current research has made limited progress on ESS discharging threshold and SOC of ESS in the URT with ESS and RES. Besides, the effort of a multi-train system with different timetables on the URT power flow has not been analyzed. Therefore, based on multi-train URT system with ESS and RES, this study investigates the effect of ESS charging threshold and different departure intervals on the URT. First, a configuration of the multi-source traction system (MSTS), which includes ESS and RES and can be directly installed in the existing traction substation, is proposed in this paper. Then, the mathematical model of URT system, ESS, and RES is introduced. After that, the energy characteristic of proposed MSTS is analyzed, and the control strategy of the MSTS has been designed to ensure the traction power supply for multi-train URT and reduce the peak power of substation. The control strategy is optimized based on the RES historical data or prediction data and traction system operation profile to achieve the better performance of the controller. In the case study, the proposed MSTS with the proposed control strategy is verified with different timetables and compared with normal URT. The main contributions of this research are:

1. Designed a coordinate control strategy for the MSTS, which can reduce the substation energy consumption, peak power, and voltage fluctuation.
2. Proposed a performance index to evaluate the substation voltage and power fluctuation and optimized the ESS control to keep the ESS remain a high SOC level.

The structure of this article is organized as follows. Section II explains the modeling of the system, including railway system model, ESS model and RES model; in Section III, the power flow analysis method is introduced first, and then the control strategy of the MSTS is designed; case studies based on multi-train system with different departure intervals are conducted in Section IV, and the proposed MSTS is compared with normal traction system via proposed performance index.

II. Modeling of Multi-source Traction System

The fundamental topology of the proposed MSTS is shown in Fig. 1 [28]. The proposed system has four main parts: (1) Railway traction substation. (2) Train vehicle. (3) Energy storage system. (4) Renewable energy. The RES unit consists of wind power and photovoltaic power, which could reduce each other's uncertainties and discontinuity due to different nature (wind power has been applied in URT) [31, 32]. The RES and ESS form a micro-grid connected to a DC busbar, and directly linked to the third rail or catenary in the traction substation. This DC busbar allows the ESS and RES to achieve the plug and play function, which has already applied in plenty of projects [33-35]. The control center receives the operation information like power and voltage of substation, power of RES, and SOC of ESS. Then, the control center sends the signal to control charging and discharging of ESS. It is worth noting that the capacity of the original transformer will not be occupied by the additional RES and ESS, which means the capacity of original substation can be improved without modification of transformer.

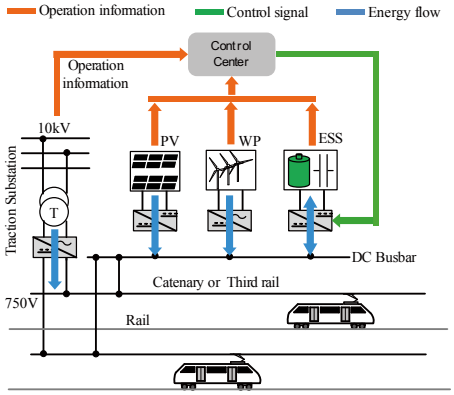

Fig. 1. Topology of the MSTS

A. Railway system modeling

1) Train Vehicle Motion Model

The urban transit has strong regularity in daily operation. So, the driving profile, like the velocity, power and position, can be calculated by the timetable and train information. To calculate the power of the train will utilize the method in [36]. Single train moving along the rail path is described by (1) [15]. The resistance force Fr can be calculated by (2).

$$\begin{cases} m_{eq}\dfrac{dv}{dt} = F_{veh} - F_r(v,s) \\ m_{eq} = m_0(1+\lambda) + m_l \\ \dfrac{ds}{dt} = v \end{cases} \tag{1}$$

$$F_r(v,s) = k_0(s) + k_1 v + k_2 v^2 \tag{2}$$

In the normal operation of urban railway transit, the train vehicle has four primary driving states: accelerating, cruising, coasting, and braking. When the train is accelerating or cruising, it obtains the traction power from the catenary, and generates the regenerative braking energy when it is decelerating. Thus, the traction power demand of the train vehicle and current can be obtained by:

$$P_{me} = F_{veh} v \tag{3}$$

$$P_{el} = \begin{cases} P_{me}/\eta & if \;\; P_{me} \geq 0 \\ P_{me}\eta & if \;\; P_{me} < 0 \end{cases} \tag{4}$$

$$I_t = \frac{P_{el}}{U_l} \tag{5}$$

2) Traction Power Network

Fig. 2 shows the equivalent circuit model of the railway traction power network. The similar modelling method can be found in [22, 23, 25]. The substation equivalent model includes a voltage source and a resistance, and the voltage of substation U_{sub} can be expressed as follow.

$$U_{sub} = U_{OC} - I_{sub} R_{sub} \tag{6}$$

The railway line is modeled as a time-varying resistance, and its value is dependent on the position of train vehicle. The traction train absorbs the power from both substations and the

braking train generates the energy for other traction trains or consumes the braking energy in braking resistance.

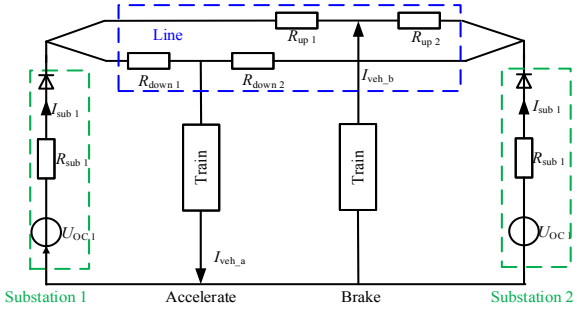

Fig. 2. The equivalent circuit model of the railway traction power network

B. ESS model

Off-board ESS is usually applied to achieve the receptivity of RBE in the charging mode, and then provide the voltage support for the catenary in the discharging mode. The ESS can be installed in substations or along the railway track. In this study, it is considered to be set in each substation. The off-board ESS has both load and generator functions.

1) ESS equivalent circuit model

The supercapacitor (SC) is considered as the ESS in this research, and its equivalent model is regarded as a resistance R and a capacitance C [24, 25, 37]. The voltage of ESS can be calculated by (8), and the state of charge of ESS is shown in (10).

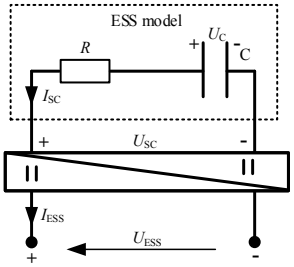

Fig. 3. ESS equivalent model

$$U_{\mathrm{C}}(t)=U_{\mathrm{C}}(0)+\frac{1}{C_{\mathrm{SC}}}\int_0^t I_{\mathrm{SC}}(\tau)d\tau \tag{7}$$

$$U_{\mathrm{SC}}(t)=U_{\mathrm{C}}(t)+R_{\mathrm{C}}I_{\mathrm{SC}}(t) \tag{8}$$

$$U_{\mathrm{ESS}}=\frac{U_{\mathrm{SC}}I_{\mathrm{SC}}}{I_{ESS}} \tag{9}$$

$$SOC(t)=\frac{U_{\mathrm{SC}}^2(t)}{U_{\mathrm{cn}}^2} \tag{10}$$

2) ESS working state

The ESS has three working states: charging, discharging and stand by. The ESS working state is determined by the substation's voltage, and the charging / discharging power of ESS will be limited according to U_{ESS} [38]. The ESS power limit for charging and discharging is shown in Fig. 4.

$P_{\mathrm{ESS\_chmax}}$ and $P_{\mathrm{ESS\_dismax}}$ represent the maximum value of charging and discharging power of ESS. In the discharging part, the ESS transfers energy to traction trains, and the maximum power of ESS will increase with the voltage of ESS in $U_1 < U_{\mathrm{ESS}} < U_3$. The ESS will not work (standby) when $U_3 < U_{\mathrm{ESS}} < U_4$. The charging mode occurs when voltage of ESS is from U_4 to U_6.

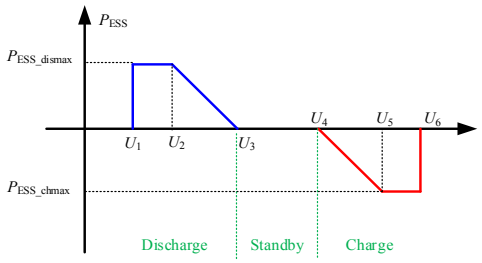

Fig. 4. Voltage-dependent power characteristic of ESS

The mathematic equations of ESS maximum discharging and charging power are expressed in (11). The $P_{\mathrm{ESS\_dis}}$ is a positive value and the $P_{\mathrm{ESS\_ch}}$ is a negative value.

$$P_{\mathrm{ESS\_max}}=\begin{cases} P_{\mathrm{ESS\_dismax}} & U_1 \le U_{\mathrm{ESS}} \le U_2 \\ P_{\mathrm{ESS\_dismax}}\dfrac{U_3-U_{\mathrm{ESS}}}{U_3-U_2} & U_2 < U_{\mathrm{ESS}} \le U_3 \\ 0 & U_3 < U_{\mathrm{ESS}} < U_4 \\ P_{\mathrm{ESS\_chmax}}\dfrac{U_{\mathrm{ESS}}-U_4}{U_5-U_4} & U_4 \le U_{\mathrm{ESS}} < U_5 \\ P_{\mathrm{ESS\_chmax}} & U_5 \le U_{\mathrm{ESS}} \le U_6 \end{cases} \tag{11}$$

To protect the ESS and avoid the deep charging and discharging action, the maximum and minimum values of ESS state of charge (SOC) are also considered here, shown in (12).

$$SOC_{\min} \le SOC \le SOC_{\max} \tag{12}$$

C. RES model

The RES unit includes wind power and photovoltaic power, which can eliminate the uncertainty of RES. The control of RES will not be considered in this research, because the objective of this research is not to control and maximize the power of RES. Thus, the RES historical data is utilized here to test the proposed MSTS.

According to the area of a normal traction substation [27], the maximum capacity of RES installed on the substation rooftop can be up to 0.5 MW. Similar to reference [31], the RES capacity is 0.25 MW in this paper, and the RES power will change from 0.05MW to 0.25 MW every 50s to reflect the fluctuation characteristic, which is shown in Fig. 5. The RES 1 and 2 is install in substation 1 and 2, respectively.

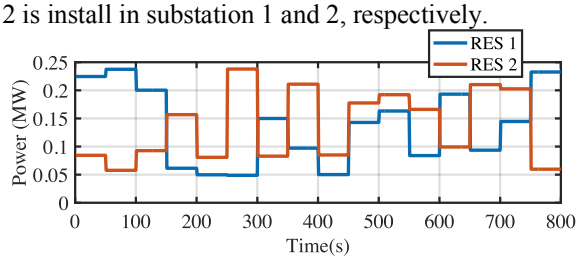

Fig. 5. Power of RES in 800s

III. Power Flow Analysis and Control Strategy

A. Power Flow Analysis

To calculate the power flow of the proposed system, the nodal voltage equation method is applied here. Since the proposed system has three stations (including two substations), the system structure can be considered as the one in Fig. 2 based on the model described in Section 2. The basic method of nodal voltage equation is similar to current research [22, 25], and the detailed equations regarding accelerating and braking trains are shown in (13) and the related equations for more trains can be obtained as well.

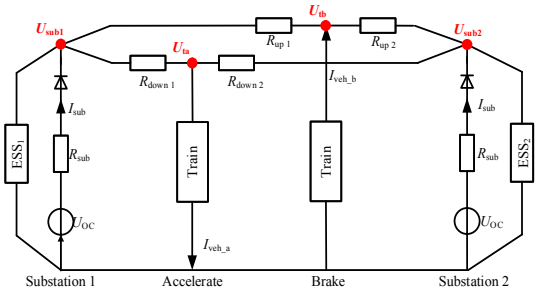

Fig. 6. The equivalent circuit of the railway system

$$\begin{cases} U_{sub1}\left(\frac{1}{R_{sub1}}+\frac{1}{R_{down1}}+\frac{1}{R_{up1}}\right)-U_{ta}\left(\frac{1}{R_{down1}}\right)-U_{tb}\left(\frac{1}{R_{up1}}\right)=I_{sub1} \\ U_{ta}\left(\frac{1}{R_{t}}+\frac{1}{R_{down1}}+\frac{1}{R_{down2}}\right)-U_{sub1}\left(\frac{1}{R_{down1}}\right)-U_{sub2}\left(\frac{1}{R_{down2}}\right)=I_{veh\_a} \\ U_{sub2}\left(\frac{1}{R_{sub2}}+\frac{1}{R_{down2}}+\frac{1}{R_{up2}}\right)-U_{ta}\left(\frac{1}{R_{down2}}\right)-U_{tb}\left(\frac{1}{R_{up2}}\right)=I_{sub2} \\ U_{tb}\left(\frac{1}{R_{t}}+\frac{1}{R_{up1}}+\frac{1}{R_{up2}}\right)-U_{sub1}\left(\frac{1}{R_{up1}}\right)-U_{sub2}\left(\frac{1}{R_{up2}}\right)=I_{veh\_b} \end{cases} \quad (13)$$

To obtain the single train operation information and multi-train system operation information, the detailed calculation method is divided into two main parts: single-train simulator and multi-train simulator. The single-train simulator, which is shown in (1) to (5), mainly obtains the train traction power demand, train regenerative braking energy, train velocity, and train location via the train movement model. In the multi-train simulator, the above results from single-train simulator will be considered together with timetable information. Then, the power and voltage of substations and catenary can be calculated via nodal voltage method in multi-train simulator. When the number of the train vehicle is more than two or less than two, the power flow can be calculated by increasing or reducing nodes and related nodal voltage equations. The overview of power flow process for the DC traction system is shown in Figure 7:

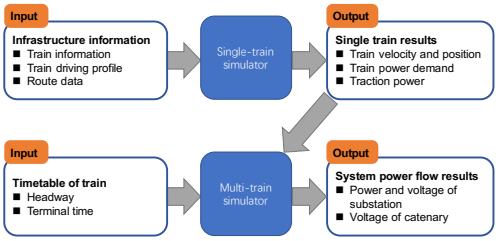

Fig. 7. Power flow calculation method

The detailed calculation step is shown below:

Step 1. Input the infrastructure information of train vehicle and traction system to single-train simulator.

Step 2. Calculate the train movement information (power, position, velocity) of a single train according to equation (1)-(3).

Step 3. Determine the departure interval and timetable.

Step 4. Initialization of the parameter of traction system.

Step 5. Input the single-train operation information, and utilize the nodal voltage equation (13) to calculate the system operation information, including power and voltage of substations.

Step 6. Output the result.

B. The operation modes of MSTS

According to the power demand from the substation, the proposed MSTS has three main operation modes as shown in Fig. 8. In operation mode (a) when the substation has available capacity, the traction substation and RES provide traction power for trains, while the RBE is transferred to accelerating trains from braking trains. The ESS works at a standby state, because the substation is capable to supply enough power. In operation mode (b), the substation power demand is high. The traction substation, RBE, ESS and RES provide traction power together. ESS is in discharging mode. In operation mode (c), the substation works in a standby mode since the RBE and RES power supply is higher than the traction power demand. RES and RBE will be transferred to charge the ESS. It is worth noting that RES will work all the time which aims to avoid curtailment of the RES power, and the ESS power is limited by the constraint described in section 2.2.

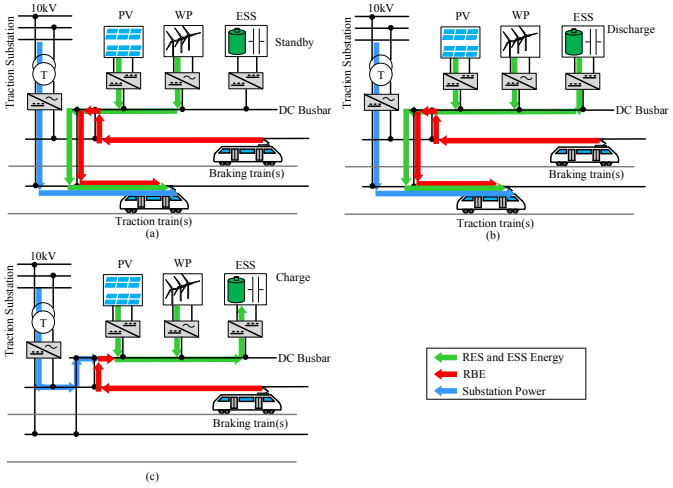

Fig. 8. Operation modes of the proposed MSTS

A part of RBE will be consumed in braking resistance when there is no train absorbing the energy and ESS SOC reaches the maximum value. So, the power of RBE can be expressed as:

$$P_{tb}=P_{b}-P_{br} \quad (14)$$

The traction power demand of train vehicle consists of power from substation and power from ESS and RES and power from RBE.

$$P_{el}=P_{sub}+P_{ESS}+P_{RES}+P_{tb} \quad (15)$$

C. Coordinated control strategy

To efficiently manage the power of each unit and reduce the energy consumption CTS, a coordinated control strategy, which considers the substation voltage, RES power, and SOC of ESS, is designed here. The proposed coordinated control strategy aims to reduce the energy consumption and peak power of substation, and stabilize the voltage of substation. Meanwhile, the decrease in RES curtailment is also taken into account. The detailed flow chart of the proposed control strategy is shown in Fig. 9. Fig. 9 (a) shows the power flow of the proposed system. The traction substation, ESS and RES will provide the power to URT, while the ESS will be charged by RES and RBE. The work state of each unit is controlled by the proposed coordinated control strategy, and there is no energy exchange between ESS and substation. To be specific, the RES will work all the time. However, the RES power may not be fully utilized when required traction power is lower than the RES power and ESS SOC has reached the maximum value.

The proposed coordinated control strategy is shown in Fig. 9 (b). For each time step, the control center will measure the substation voltage, and decide the RES work state. If the substation voltage is larger than open-circuit voltage of substation, the RES will not provide the traction power, while the ESS will be charged by RES and RBE. On the contrary, the RES will participate in the traction power supply when the substation voltage is lower than the open-circuit voltage. Then, decide the ESS work state by comparing the voltage of substation with voltage threshold. The voltage threshold is optimized according to URT operation data, ESS parameter and RES historical data, and the calculation method will be introduced later. The ESS will provide the traction power together with substation and RES when substation voltage is lower than the voltage threshold. If the substation voltage does not reach the threshold value, the ESS will be in a standby state.

In this proposed control strategy, the RES will take part in traction power supply. Besides, ESS can provide traction power to reduce the peak power of substation when substation output power reaches the defined threshold value. As for ESS charging, RES and RBE will transfer energy to ESS when substation does not work in traction mode. Thanks to this strategy, the peak power of substation can be reduced, and the capacity of substation can be improved by adjusting the ESS discharging threshold. Meanwhile, the voltage range of substation will be decreased due to external power source.

It is worthy to note that when ESS discharges and charges, it should satisfy the principle shown in Fig. 4, and the power of ESS will not exceed its maximum value. The ESS will discharge and provide the traction power when the peak power of substation is high. However, the SOC of ESS will be below the minimum value when it provides overmuch power, due to its limited capacity. Thus, the ESS discharge threshold should be considered according to the situation of the whole system.

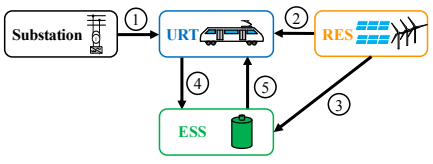

(a)

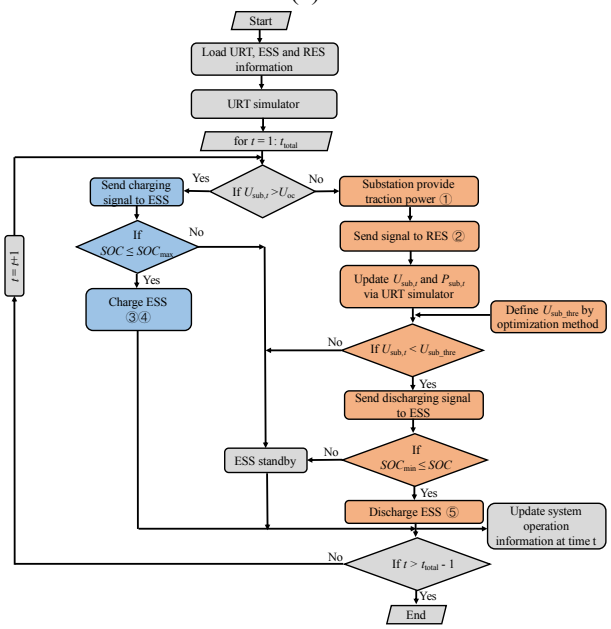

(b)

Fig. 9. System control strategy: (a) Energy flow chart (b) Coordinated control strategy

D. ESS control Optimization

To achieve a better performance of the proposed coordinated control strategy, the ESS discharging threshold need to be adjusted according to different scenarios. The charging threshold will not be optimized because the ESS SOC needs to be remained at a high level. The peak power and voltage range of substations are the main indexes of URT operation. Thus, define a performance index J_1, J_2, and J_3 shown in (16). α and β are the weight of performance index, and $\alpha+\beta=1$:

$$J = \alpha J_1 + \beta (J_2 + J_3) \tag{16}$$

The J_1, J_2, and J_3 are shown as follows:

$$\begin{cases} J_1 = \sum_{i=1}^{n} \dfrac{\int_0^T \left(P_{\text{sub\_os},i}(t) - P_{\text{sub\_up}} \right) dt}{T P_{\text{sub\_up}}} \\ J_2 = \sum_{i=1}^{n} \dfrac{\int_0^T \left(U_{\text{sub\_os},i}(t) - U_{\text{sub\_up}} \right) dt}{T U_{\text{sub\_up}}} \\ J_3 = \sum_{i=1}^{n} \dfrac{\int_0^T \left(U_{\text{sub\_down}} - U_{\text{sub\_us},i}(t) \right) dt}{T U_{\text{sub\_down}}} \end{cases} \tag{17}$$

$P_{\text{sub\_up}}$, $U_{\text{sub\_up}}$, and $U_{\text{sub\_down}}$ are fixed values (shown in Fig. 10) of substation power and voltage, which are chosen as the benchmark of the overshoot and undershoot.

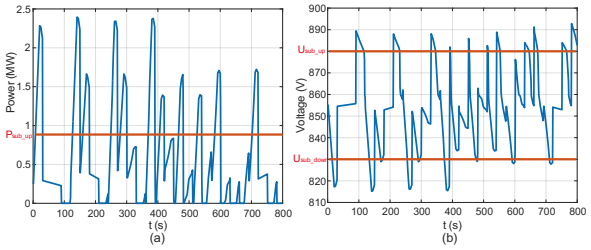

Fig. 10. Defined value of performance index

The benchmark is chosen according to the traction system information. The power benchmark is chosen by (18), and the voltage benchmarks are chosen as (19) and (20).

$$P_{\text{sub\_up}} = P_{\text{peak}} - P_{\text{ESS\_max}} \tag{18}$$

$$U_{\text{sub\_up}} = U_4 \tag{19}$$

$$U_{\text{sub\_down}} = U_{\text{OC}} + \frac{1}{2}\sqrt{(U_{\text{OC}}^2 - 4R_{\text{sub}}P_{\text{sub\_up}})} \tag{20}$$

Where P_{peak} is the peak power of each substation which can be obtained by the convention traction system simulation, U_4 is the ESS charging trigger voltage.

The objective function is set as minimizing the sum of J_1, J_2, and J_3:

$$\text{Minimize } J = \alpha J_1 + \beta(J_2 + J_3) \tag{21}$$

The particle swarm optimization (PSO) is applied here to optimize the ESS charging threshold, because the PSO has been widely used in parameter optimization problem [39-44], and the PSO can meet the speed and accuracy requirement. The daily operation information of URT, parameter of ESS, and historical data of RES will be used to optimize the ESS discharging threshold by the above optimization method. The detailed process of optimization will not be discussed here.

IV. Case Study and Analysis

A. Parameter Setting

1) Topology of the simulation system

A comparison between the conventional traction system (CTS) and MSTS will be conducted. The topology of simulation system is shown in Fig. 11. The CTS has the same structure, but the PV, WP, and ESS are not considered.

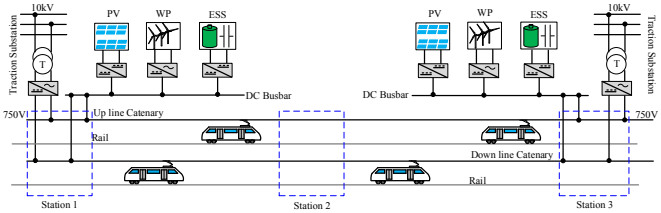

Fig. 11. Topology of the Simulation System

2) Main Parameters

The main parameters of urban railway system and ESS are shown in TABLE I and TABLE II.

TABLE I
PARAMETERS OF THE RAILWAY SYSTEM

L	1750 m	Headway	2/5 mins
R_l	0.016 Ω/km	Train type	3M3T
R_t	0.015 Ω	m_{eq}	210 t
U_{b_rate}	825 V	U_{t_rate}	750 V
R_{sub}	0.0161 Ω	P_{au}	90 kW
U_{oc}	860 V		

TABLE II
PARAMETERS OF THE ESSS (SUPERCAPACITOR)

C_{ESS}	294 F	U_{ESS_rate}	750 V
P_{ESS_rate}	1.5 MW	E_{ESS_total}	8.4 kWh
SOC_{max}	0.9	$SOC_{initial}$	0.9/0.8
SOC_{min}	0.2	U_1/U_2	800/820V
$U_4/U_5/U_6$	870/880/920 V		

3) Driving Profile and Timetable

Fig. 12 shows the traction power of the single train, and the velocity of the train is in accelerating, cruising, coasting, and braking mode, respectively.

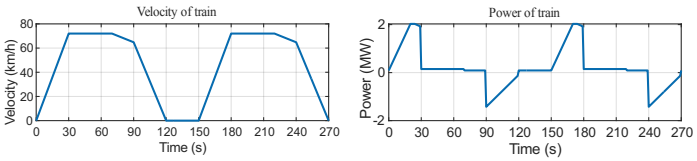

Fig. 12. Traction power and velocity of the train vehicle

Both upline and downline have train vehicles operating in the railway system, the simulation period is chosen as 800 seconds. In Fig. 13, two timetables with different departure intervals are applied here, including 120s for peak period and 300s for off-peak period.

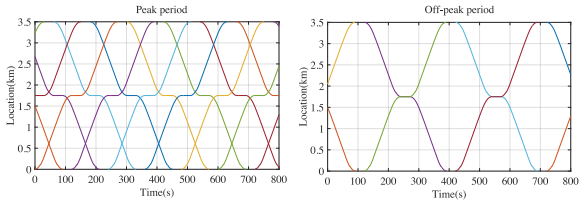

Fig. 13. Timetable of peak and off-peak period

Considering the uncertainty of RES, the RES is set as Fig. 5, which is similar to the reference [31]. The main objective of this research is not to maximize the RES power, so the RES output power is directly connected to the DC bus bar. Both RESs are assumed to change randomly every 50s, and the maximum power is 0.24 MW.

4) ESS Optimization parameter setting

The benchmark of substation power and voltage is shown in TABLE III, and the weight of performance index is chosen as 0.5 and 0.5, considering power and voltage have same weight. The PSO's population is 50, maximum iteration is 100.

TABLE III
PARAMETERS OF PERFORMANCE INDEX

Index	Peak period	Off-peak period
P_{sub_up}	1.09 MW	1.82 MW
U_{sub_up}	870 V	870 V
U_{sub_down}	771.75 V	824.45 V

B. Results and Analysis

Based on the setting in Section 4.1, the case study firstly analyzed the substation performance of conventional traction system (CTS) in two different departure intervals. Then, the CTS with ESS and multi-source traction system (MSTS) are compared under the proposed coordinated control strategy. At last, the MSTS is tested in long-term operation, and the system robustness is verified by extreme situation of RES.

1) Scenario A: Power analysis of CTS

In this scenario, the CTS is investigated under different departure intervals. The comparison between two departure intervals, which stand for the peak period and off-peak period respectively, is conducted here. Fig. 14 illustrates the operation

information, including power and voltage of substations in CTS.

In Fig. 14, it can be obtained that both substation 1 and 2 peak power exceed 2.5 MW. The substation power keeps at a high value in peak period, while the substation power has a highest value (3.32MW) in off-peak period. The voltage range of substations is from 812 V to 981 V in peak period, while the range is from 797.85 V to 1000 V in off-peak period. In off-peak period, substations can reach a lower and higher voltage value than the one in peak period, because RBE is consumed in braking resistance rather than being transferred to other trains.

TABLE IV
RESULT OF CTS AND CTS WITH ESS AND MSTS

Period	System	Peak power (MW) Substation 1/2	Maximum Voltage (V) Substation 1/2	Minimum Voltage(V) Substation 1/2	SOC ESS 1/2
Peak	CTS	2.58/2.59	981.55/978.43	811.78/811.54	\
	CTS with ESS	2.20/2.20	885.60/884.84	816.62/816.62	0.39/0.32
	MSTS	1.85/1.85	885.60/884.84	823.85/823.85	0.38/0.39
Off-peak	CTS	3.26/3.32	1000/1000	798.63/798.16	\
	CTS with ESS	1.85/1.85	899.48/899.49	823.85/823.85	0.56/0.53
	MSTS	1.75/1.75	889.48/899.49	825.89/825.89	0.60/0.62

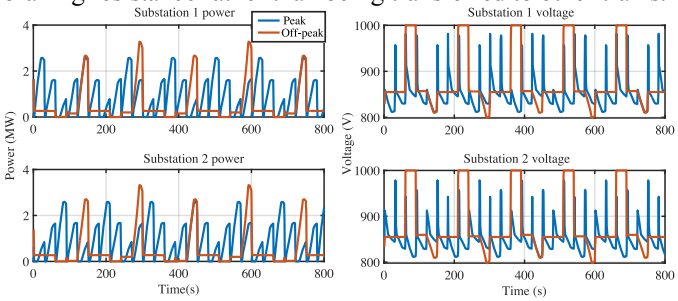

Fig. 14. Operation information of substations

2) Scenario B: Comparison between CTS with ESS and MSTS

In this scenario, the proposed MSTS with coordinated control strategy is investigated here by comparing the system dynamic response of the CTS with ESS and. Both peak and off-peak period are considered, and the RES in MSTS is simulated as Fig. 5 which is referred to research [31]. The result of ESS discharging threshold optimization is shown in TABLE V.

TABLE V
OPTIMIZATION RESULT OF ESS DISCHARGING THRESHOLD

System	Period	Threshold
CTS with ESS	Peak	816.63 V
	Off-peak	823.81 V
MSTS (ESS and RES)	Peak	823.85 V
	Off-peak	825.89 V

The operation information of substation 1 and ESS 1 in peak period can be seen in Fig. 15. Due to RES providing a part of traction power, the substation peak power has been furtherly reduced compared to CTS with ESS. The peak power of substation 1 is 1.85MW MSTS, compared with 2.20 MW in CTS with ESS. The voltage drop in MSTS is also less than the one in CTS with ESS, decreasing from 884.84 V to 823.85 V. As for work state of ESS 1, the charging power is larger than the one in CTS with ESS, while it also exports more discharging power, and the SOC of ESS 1 can still be larger than minimal value in MSTS. The substation 2 and ESS 2 has similar result, which is not shown here, and the detailed data for CTS, CTS with ESS and MSTS is summarized in TABLE IV.

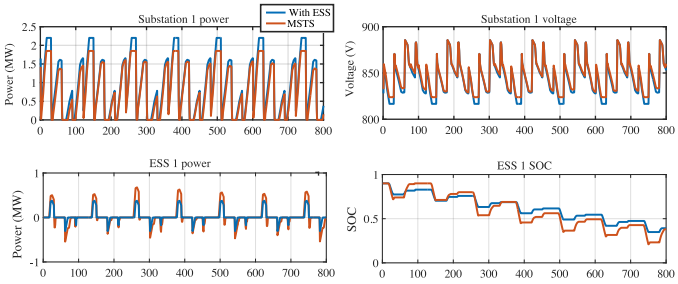

Fig. 15. Simulation result of substation 1

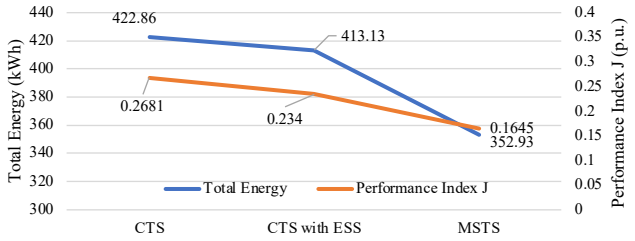

Fig. 16. System comparison in peak period

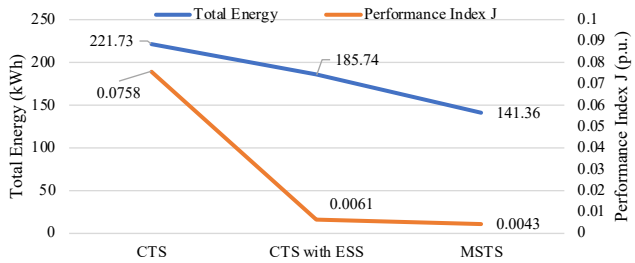

Fig. 17. System comparison in off-peak period

Compared with CTS, it can be obtained that the MSTS decreases 16.54% and 36.25% energy consumption from the utility grid during peak and off-peak period, respectively. In terms of proposed performance index J, the proposed MSTS has superior performance among three systems, improving 38.64% in peak period and 94.32% in off-peak. Other detailed comparison between CTS with ESS and MSTS is shown in TABLE IV. The maximum voltages of each substation are same in CTS with ESS and MSTS, because they both have the ESS to absorb the RBE. The result illustrates that the combination of ESS and RES can improve the utilization rate of ESS and

reduce the peak power and voltage fluctuation of traction substation.

3) Scenario C: Long-term operation analysis

To further investing the proposed MTST and its coordinated control strategy, a long-term simulation is conducted here from 6:00 to 12:00 (6:00 to 9:00 represents the peak period and 9:00 to 12:00 represents the off-peak period, and departure interval is same as the one shown in Fig. 13). The ESS discharging threshold is optimized respectively according to timetable and RES historical data, and the result is 819.53 V (peak period) and 826.29 V (off-peak period). The historical data of RES is considered as

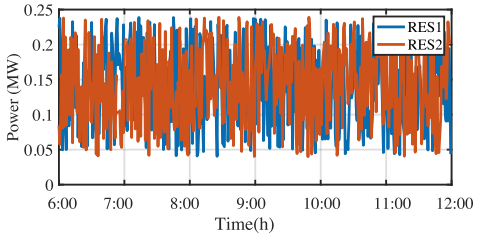

Fig. 18. RES power in long-term simulation

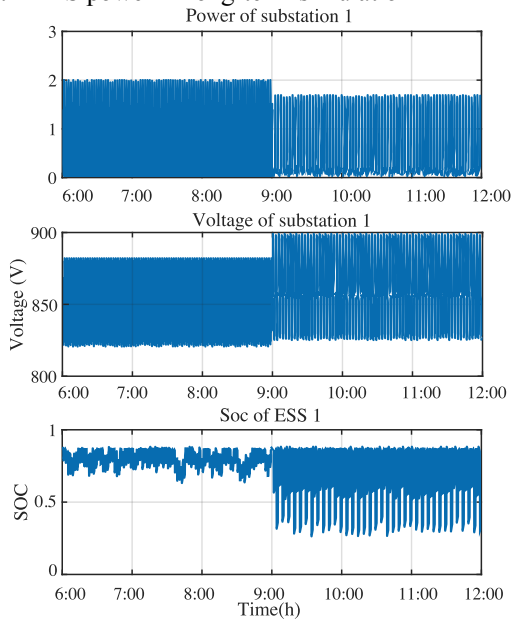

Fig. 19. Simulation results of substation 1

The simulation result of substation 1 is shown in Fig. 19, where it shows that the peak power of substation 1 is kept below 2.05 MW and 1.70 MW in peak and off-peak period, respectively. The voltage fluctuation is also remained from 817.9 V to 885.6 V and 826.9 V to 899.98 V in peak and off-peak period. The SOC of ESS 1 is kept above the minimum value which ensure the ESS has enough energy to provide the traction power. As for the power and voltage of substation 2 has the similar result with substation 1, which is not shown here.

The energy consumption and performance index comparisons between CTS and MSTS in long-term simulation are conducted here and the result is shown in Fig. 20. The total energy consumption of MSTS is 6839.7 kWh which reduces 22.8 % energy consumption compared with CTS between 6:00 to 12:00. The performance index of MSTS is also decreased 45.1 %.

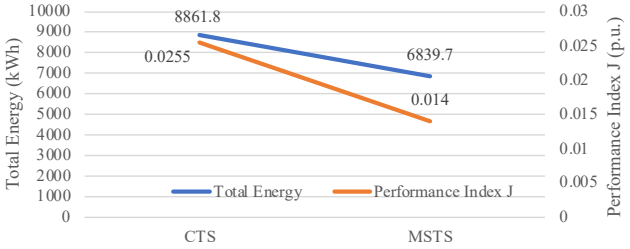

Fig. 20. System comparison in long-term simulation

4) Scenario D: System robustness analysis

This section aims to test the sensitivity of proposed MSTS and coordinated control strategy under extreme situations like the output of RES reduces to zero caused by the weather condition or machine fault. Based on the long-term simulation in Section 4.2.3, it is supposed that the output of RES drops to zero for 5 minutes, from 7:00 to 7:05 and from 10:30 to 10:35 in peak and off-peak period, respectively. The operation result of substation 1 and ESS 1 is shown in Fig. 21.

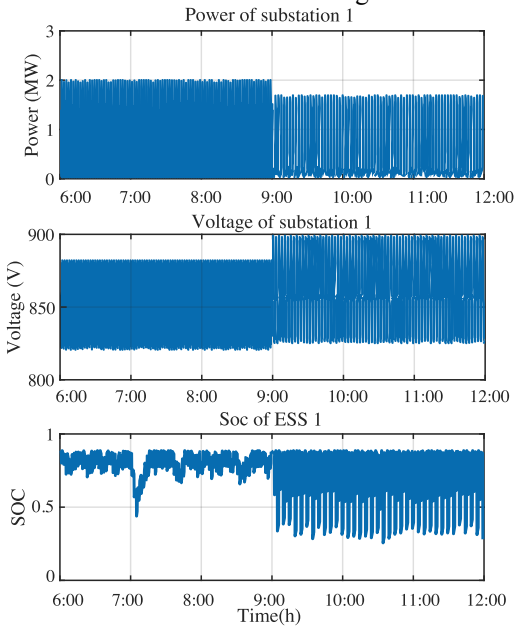

Fig. 21. Simulation result of substaiton 1 when RES stops for 5 minutes

The result shows that the substation 1 peak power and minimum voltage still remain the same when RES drops to zero, because the ESS provides the required power. Regarding the SOC of ESS, a drop from 0.83 to 0.45 can be observed when RES power equals to zero in peak period and a slightly drop (from 0.29 to 0.26) in off-peak period, which ensures that ESS 1 has enough SOC to provide the traction power (Substation 2 and ESS 2 have the similar result which are not shown here). The proposed MSTS has the robustness when RES drops to zero for 5 minutes in peak and off-peak period.

To furtherly investigate the system robustness, it is supposed that the output of RES drops to zero from 7:00 to 7:10 and from 10:30 to 10:40 in peak and off-peak period, respectively. The operation result of substation 1 and ESS 1 is shown in Fig. 22.

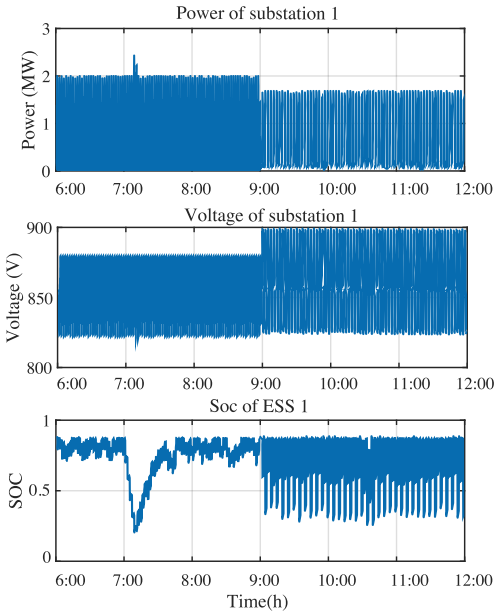

Fig. 22. Simulation result of substaiton 1 when RES stops for 10 minutes

The power of substation 1 increases 21.95 % when RES stops in peak period, while the power increases 2.89 % in off-peak period. The peak power of substation is still under the maximum value and reduces to previous states when RES works again. The voltage sag occurs when RES stops, reaching 810.40 V and 825.31 V in peak and off-peak period, respectively. As for ESS 1 work state, the SOC of ESS 1 drops to the minimum value when RES stops. However, the SOC can still go back to a high level which reduces the substation peak power. Substation 2 has the similar result which is not shown here.

Thus, the proposed MSTS with the coordinated control strategy can still reduce the peak power and voltage fluctuation and remain the SOC of ESS when facing extreme situations like RES power drops to zero. Namely, the proposed MSTS with the coordinated control strategy has certain robustness. Besides, improving the capacity of ESS can enhance the robustness of system.

V. Conclusion

This research proposes a multi-source traction system, which can achieve the plug and play of ESS and RES due to the DC busbar. After building the equivalent model of railway system and ESS, the energy flow calculation method is designed, and the energy distribution is analyzed. Then, a coordinated control strategy is proposed to manage the work state of RES and ESS according to the voltage of substations, including an optimization method of ESS discharging threshold with system performance index. The case study is conducted based on three stations (including two substations), multiple trains, and different departure intervals, considering peak period and off-peak period. The influence of departure interval is analyzed first in the case study, which demonstrates that peak power will increase in the peak period and voltage fluctuation will be more severe in off-peak period. Then, the MSTS is tested in short-term and long-term simulation, compared with CTS equipped with ESS. Both results show the proposed MSTS with the coordinated control strategy can reduce the peak power and voltage sag, and the substation capacity can be improved because of the decreasing peak power. In long-term simulation, the MSTS save 22.8 % energy consumption from substation compared with CTS. Besides, the robustness of the MSTS is verified by simulating extreme situations like RES fault. The proposed MSTS with coordinated control strategy can be applied in a full railway line, solving with more simulation time and nodal voltage equations. However, the proposed coordinated control strategy needs to be designed separately for scenarios with different departure intervals, and other factors like the effect of the passenger's quantity are not considered. The future research will consider a more detailed modelling method, and the real-time control strategy will be applied to cope with the uncertainty of the system. Besides, ESS will also be charged by substation to achieve an economy operation. At last, the system will be tested in a hardware-in-loop system with actual railway system data.

VI. References

[1] S. Wandelt, Z. Wang, and X. Sun, "Worldwide Railway Skeleton Network: Extraction Methodology and Preliminary Analysis," *IEEE Transactions on Intelligent Transportation Systems,* vol. 18, no. 8, pp. 2206-2216, 2017.

[2] F. Meng, G. Liu, Z. Yang, M. Casazza, S. Cui, and S. Ulgiati, "Energy efficiency of urban transportation system in Xiamen, China. An integrated approach," *Applied energy,* vol. 186, pp. 234-248, 2017.

[3] H. Xiufang, M. Jianping, Z. Chao, and L. Gaoyuan, "Statistics and Analysis of Urban Rail Transit in 2019," *URBAN RAPID RAIL TRANSIT,* vol. 33, no. 4, pp. 1-8, Aug 2019.

[4] D. I. Fletcher, R. F. Harrison, and S. Nallaperuma, "TransEnergy – a tool for energy storage optimization, peak power and energy consumption reduction in DC electric railway systems," *Journal of Energy Storage,* vol. 30, p. 101425, 2020/08/01/ 2020. [Online]. Available: https://www.sciencedirect.com/science/article/pii/S2352152X19315026.

[5] I. Amit and D. Goldfarb, "The timetable problem for railways," *New York, NY, USA: Gordon and Breach, ,* pp. 379–387, 1971.

[6] Y. Bai, Y. Cao, Z. Yu, T. K. Ho, C. Roberts, and B. Mao, "Cooperative Control of Metro Trains to Minimize Net Energy Consumption," *IEEE Transactions on Intelligent Transportation Systems,* vol. 21, no. 5, pp. 2063-2077, 2020.

[7] X. Yang, B. Ning, X. Li, and T. Tang, "A Two-Objective Timetable Optimization Model in Subway Systems," *IEEE Transactions on Intelligent Transportation Systems,* vol. 15, no. 5, pp. 1913-1921, 2014.

[8] L. Xiang, D. Wang, K. Li, and Z. Gao, "A green train scheduling model and fuzzy multi-objective optimization algorithm," *Applied Mathematical Modelling,* vol. 37, no. 4, pp. 2063-2073, 2013.

[9] R. R. Liu and I. M. Golovitcher, "Energy-efficient operation of rail vehicles," *Transportation Research Part A,* vol. 37, no. 10, pp. 917-932, 2003.

[10] Z. Tian, N. Zhao, S. Hillmansen, C. Roberts, T. Dowens, and C. Kerr, "SmartDrive: Traction Energy Optimization and Applications in Rail Systems," *IEEE Transactions on Intelligent Transportation Systems,* vol. 20, no. 7, pp. 2764-2773, 2019.

[11] B. Ke, C. Lin, and C. Yang, "Optimisation of train energy-efficient operation for mass rapid transit systems," *IET Intelligent Transport Systems,* vol. 6, no. 1, pp. 58-66, 2012.

[12] S. Lu, S. Hillmansen, T. K. Ho, and C. Roberts, "Single-Train Trajectory Optimization," *IEEE Transactions on Intelligent Transportation Systems,* vol. 14, no. 2, pp. 743-750, 2013.

[13] S. Su, X. Li, T. Tang, and Z. Gao, "A Subway Train Timetable Optimization Approach Based on Energy-Efficient Operation Strategy," *IEEE Transactions on Intelligent Transportation Systems,* vol. 14, no. 2, pp. 883-893, 2013.

[14] S. Su, X. Wang, Y. Cao, and J. Yin, "An Energy-Efficient Train Operation Approach by Integrating the Metro Timetabling and Eco-Driving," *IEEE Transactions on Intelligent Transportation Systems,* vol. 21, no. 10, pp. 4252-4268, 2020.
[15] M. Blanco-Castillo, A. Fernández-Rodríguez, A. Fernández-Cardador, and A. P. Cucala, "Eco-Driving in Railway Lines Considering the Uncertainty Associated with Climatological Conditions," *Sustainability (Switzerland),* Article vol. 14, no. 14, 2022, Art no. 8645.
[16] K. Minaminosono, M. Hashimoto, and T. Yoshinaga, "Study of Potential and Utilization of Regenerative Power in Electric Railway," in *2019 8th International Conference on Renewable Energy Research and Applications (ICRERA)*, 3-6 Nov. 2019 2019, pp. 164-168.
[17] V. Calderaro, V. Galdi, G. Graber, and A. Piccolo, "Siting and sizing of stationary SuperCapacitors in a Metro Network," in *AEIT Annual Conference 2013*, 3-5 Oct. 2013 2013, pp. 1-5.
[18] D. Roch-Dupré, T. Gonsalves, A. P. Cucala, R. R. Pecharromán, Á. J. López-López, and A. Fernández-Cardador, "Determining the optimum installation of energy storage systems in railway electrical infrastructures by means of swarm and evolutionary optimization algorithms," *International Journal of Electrical Power & Energy Systems,* vol. 124, p. 106295, 2021/01/01/ 2021.
[19] P. Liu, L. Yang, Z. Gao, Y. Huang, S. Li, and Y. Gao, "Energy-Efficient Train Timetable Optimization in the Subway System with Energy Storage Devices," *IEEE Transactions on Intelligent Transportation Systems,* vol. 19, no. 12, pp. 3947-3963, 2018.
[20] S. Nallaperuma, D. Fletcher, and R. Harrison, "Optimal control and energy storage for DC electric train systems using evolutionary algorithms," *Railway Engineering Science,* vol. 29, no. 4, pp. 327-335, 2021.
[21] Q. Qin, T. Guo, F. Lin, and Z. Yang, "Energy Transfer Strategy for Urban Rail Transit Battery Energy Storage System to Reduce Peak Power of Traction Substation," *IEEE Transactions on Vehicular Technology,* vol. 68, no. 12, pp. 11714-11724, 2019.
[22] Z. Yang, Z. Yang, H. Xia, and F. Lin, "Brake Voltage Following Control of Supercapacitor-Based Energy Storage Systems in Metro Considering Train Operation State," *IEEE Transactions on Industrial Electronics,* vol. 65, no. 8, pp. 6751-6761, 2018.
[23] F. Zhu, Z. Yang, H. Xia, and F. Lin, "Hierarchical Control and Full-Range Dynamic Performance Optimization of the Supercapacitor Energy Storage System in Urban Railway," *IEEE Transactions on Industrial Electronics,* vol. 65, no. 8, pp. 6646-6656, 2018.
[24] F. Zhu, Z. Yang, F. Lin, and Y. Xin, "Decentralized Cooperative Control of Multiple Energy Storage Systems in Urban Railway Based on Multiagent Deep Reinforcement Learning," *IEEE Transactions on Power Electronics,* vol. 35, no. 9, pp. 9368-9379, 2020.
[25] Z. Yang, F. Zhu, and F. Lin, "Deep-Reinforcement-Learning-Based Energy Management Strategy for Supercapacitor Energy Storage Systems in Urban Rail Transit," *IEEE Transactions on Intelligent Transportation Systems,* vol. 22, no. 2, pp. 1150-1160, 2021.
[26] S. Boudoudouh and M. Maâroufi, "Smart control in a DC railway by Multi Agent System (MAS)," in *2016 International Conference on Electrical Systems for Aircraft, Railway, Ship Propulsion and Road Vehicles & International Transportation Electrification Conference (ESARS-ITEC)*, 2-4 Nov. 2016 2016, pp. 1-6.
[27] Y. Ishii *et al.*, "A Study of Introduction of the Photovoltaic Generation System to Conventional Railway," in *2019 8th International Conference on Renewable Energy Research and Applications (ICRERA)*, 3-6 Nov. 2019 2019, pp. 1003-1007.
[28] M. Brenna, F. Foiadelli, and H. J. Kaleybar, "The Evolution of Railway Power Supply Systems Toward Smart Microgrids: The concept of the energy hub and integration of distributed energy resources," *IEEE Electrification Magazine,* vol. 8, no. 1, pp. 12-23, 2020.
[29] M. Fleck, S. Khayyam, and A. Monti, "Day-ahead optimization for railway energy management system," in *2016 International Conference on Electrical Systems for Aircraft, Railway, Ship Propulsion and Road Vehicles & International Transportation Electrification Conference (ESARS-ITEC)*, 2-4 Nov. 2016 2016, pp. 1-8.
[30] L. Razik, N. Berr, S. Khayyam, F. Ponci, and A. Monti, "REM-S–Railway Energy Management in Real Rail Operation," *IEEE Transactions on Vehicular Technology,* vol. 68, no. 2, pp. 1266-1277, 2019.
[31] S. Boudoudouh and M. Maaroufi, "Renewable Energy Sources Integration and Control in Railway Microgrid," *IEEE Transactions on Industry Applications,* vol. 55, no. 2, pp. 2045-2052, 2019.
[32] B. Celik, A. Verdicchio, and T. Letrouvé, "Sizing of renewable energy and storage resources in railway substations according to load shaving level," in *2020 IEEE Vehicle Power and Propulsion Conference (VPPC)*, 18 Nov.-16 Dec. 2020 2020, pp. 1-5.
[33] J. Chen, S. Yan, T. Yang, S. C. Tan, and S. Y. Hui, "Practical Evaluation of Droop and Consensus Control of Distributed Electric Springs for Both Voltage and Frequency Regulation in Microgrid," *IEEE Transactions on Power Electronics,* vol. 34, no. 7, pp. 6947-6959, 2019.
[34] K. Lai and L. Zhang, "Sizing and Siting of Energy Storage Systems in a Military-Based Vehicle-to-Grid Microgrid," *IEEE Transactions on Industry Applications,* vol. 57, no. 3, pp. 1909-1919, 2021.
[35] L. Meng, T. Dragicevic, and J. M. Guerrero, "Adaptive Control Design for Autonomous Operation of Multiple Energy Storage Systems in Power Smoothing Applications," *IEEE Transactions on Industrial Electronics,* vol. 65, no. 8, pp. 6612-6624, 2018.
[36] H. Novak, V. Lešić, and M. Vašak, "Hierarchical Model Predictive Control for Coordinated Electric Railway Traction System Energy Management," *IEEE Transactions on Intelligent Transportation Systems,* vol. 20, no. 7, pp. 2715-2727, 2019.
[37] N. Devillers, S. Jemei, M.-C. Péra, D. Bienaimé, and F. Gustin, "Review of characterization methods for supercapacitor modelling," *Journal of Power Sources,* vol. 246, pp. 596-608, 2014/01/15/ 2014.
[38] P. Arboleya, B. Mohamed, and I. El-Sayed, "DC Railway Simulation Including Controllable Power Electronic and Energy Storage Devices," *IEEE Transactions on Power Systems,* vol. 33, no. 5, pp. 5319-5329, 2018.
[39] Anamika, R. Peesapati, and N. Kumar, "Electricity Price Forecasting and Classification Through Wavelet–Dynamic Weighted PSO–FFNN Approach," *IEEE Systems Journal,* vol. 12, no. 4, pp. 3075-3084, 2018.
[40] M. Veerachary and A. R. Saxena, "Optimized Power Stage Design of Low Source Current Ripple Fourth-Order Boost DC–DC Converter: A PSO Approach," *IEEE Transactions on Industrial Electronics,* vol. 62, no. 3, pp. 1491-1502, 2015.
[41] M. Zouari, N. Baklouti, J. Sanchez-Medina, H. M. Kammoun, M. B. Ayed, and A. M. Alimi, "PSO-Based Adaptive Hierarchical Interval Type-2 Fuzzy Knowledge Representation System (PSO-AHIT2FKRS) for Travel Route Guidance," *IEEE Transactions on Intelligent Transportation Systems,* vol. 23, no. 2, pp. 804-818, 2022.
[42] S. Javed, K. Ishaque, S. A. Siddique, and Z. Salam, "A Simple Yet Fully Adaptive PSO Algorithm for Global Peak Tracking of Photovoltaic Array Under Partial Shading Conditions," *IEEE Transactions on Industrial Electronics,* vol. 69, no. 6, pp. 5922-5930, 2022.
[43] X. Su, M. A. S. Masoum, and P. J. Wolfs, "PSO and Improved BSFS Based Sequential Comprehensive Placement and Real-Time Multi-Objective Control of Delta-Connected Switched Capacitors in Unbalanced Radial MV Distribution Networks," *IEEE Transactions on Power Systems,* vol. 31, no. 1, pp. 612-622, 2016.
[44] J. Yang, H. Dong, Y. Huang, L. Cai, F. Gou, and Z. He, "Coordinated optimization of vehicle-to-grid control and load frequency control by considering statistical properties of active power imbalance," *International Transactions on Electrical Energy Systems,* vol. 29, no. 3, p. e2750, 2019.

Hongzhi Dong (Student Member, IEEE) received the B.S. and M.S. degrees in School of electrical engineering, Southwest Jiaotong University in 2016 and 2019. He is currently a PhD student in the Department of Electrical Engineering and Electronics at the University of Liverpool. His research interests include analysis and control of power system, modelling and optimization of railway system with renewable energy.

Zhongbei Tian (Member, IEEE) received the B.Eng in Huazhong University of Science and Technology, Wuhan, China, in 2013. He received the B.Eng. and PhD degree in Electrical and Electronic Engineering from the University of Birmingham, Birmingham, U.K., in 2013 and 2017. He is currently a Lecturer in Electrical Energy Systems at the University of Liverpool. His research interests include railway traction power system modelling and analysis, energy-efficient train control, energy system optimization, and

sustainable transport energy systems integration and management.

Joseph W. Spencer received the B.Eng. and Ph.D. degrees in electrical engineering from the University of Liverpool, Liverpool, U.K., in 1981 and 1984, respectively. He is a Professor of Electrical Engineering, the Director of the Centre for Intelligent and Monitoring Systems, and was the Head of the School of Electrical Engineering, Electronics and Computer Science with the University of Liverpool. His current research interests include electrical power equipment and intelligent monitoring systems. Prof. Spencer is a Committee Member of the British Standards Institution and a Fellow of the Institution of Electrical Engineering, U.K.

David Fletcher is Professor of Railway Engineering in the Department of Mechanical Engineering at the University of Sheffield in the United Kingdom. He received his PhD from Sheffield in 1999, and his undergraduate Mechanical Engineering degree from the University of Leeds. Over the past ten years he has been active in research on energy demand reduction and most recently application of energy storage for electrified railway networks. He is active in rail electrification research on the pantograph to overhead line interface, and has focused on a network modelling approach to build on his experience in modelling mechanical aspects of train to infrastructure interaction.

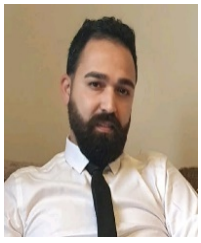

Siavash Hajiabady received the B.Eng in Electrical and Energy Engineering from the University of Birmingham, U.K., in 2011. and Master of Research in Railways Systems engineering and Integration from the University of Birmingham, U.K., in 2013 and also, and PhD degree on condition monitoring of the power converter and gearbox of wind turbines from the University of Birmingham, U.K., in 2018. He is currently a Distribution Engineer at the Network Rail. His research interests include railway traction power system modelling and analysis and green energy supply for the Railway.